Scientific Research Publishing

Advances in Nanoparticles, 2023, 12, 22-31
https://www.scirp.org/journal/anp
ISSN Online: 2169-0529
ISSN Print: 2169-0510

Improved Catalytic Reaction of Biotemplated Palladium Nanoparticles through Immobilized Metal Affinity Purification

Shadrach Ibinola, Hazim Aljewari, Imann Mosleh, Robert Beitle*

Ralph E. Martin Department of Chemical Engineering, University of Arkansas, Fayetteville, USA
Email: *rbeitle@uark.edu

How to cite this paper: Ibinola, S., Aljewari, H., Mosleh, I. and Beitle, R. (2023) Improved Catalytic Reaction of Biotemplated Palladium Nanoparticles through Immobilized Metal Affinity Purification. *Advances in Nanoparticles*, **12**, 22-31.
https://doi.org/10.4236/anp.2020.121003

Received: December 9, 2022
Accepted: February 5, 2023
Published: February 8, 2023

Copyright © 2023 by author(s) and Scientific Research Publishing Inc.
This work is licensed under the Creative Commons Attribution International License (CC BY 4.0).
http://creativecommons.org/licenses/by/4.0/

Open Access

Abstract

To investigate the effect purification plays on nanoparticle (NP) synthesis and catalytic activity, three copies of Pd4 (TSNAVHPTLRHL) fused to the N-terminus of Green Fluorescent Protein (GFP) was produced recombinantly and its characteristics pre and post purification was assessed. An *E. coli* expression system was employed, and purification was performed with Immobilized Metal Affinity Column (IMAC). Transmission electron microscopy (TEM) was utilized to examine the morphology of NPs synthesized with an enriched protein sample and ImageJ was used to determine the average size to be 2.44 nm. The turnover frequency of fabricated NP from the purified protein was analyzed by a model Suzuki-Miyaura coupling reactions and determined to be 33,000 hr^{-1}. This value is three times higher than the turnover frequency when crude lysate containing $(Pd4)_3$-GFP was used during NP synthesis. This result shows that enrichment enhanced the catalytic activity of NP.

Keywords

Protein Expression, Nanoparticle Synthesis, Turnover Frequency, Suzuki-Miyaura

1. Introduction

In recent years, researchers have looked to nature for alternative ways to fabricate nanoparticles (NPs). Nanoparticle synthesis is characterized into two categories which are top-down and bottom up [1]. Nanoparticles are used in various applications which include coatings, nanofibers, textiles [2] [3] [4] [5] [6] and catalysts in fuel cells and pharmaceutical production [7] [8]. Milling and attrition are the main top-down methods which are more labor intensive and pro-

duce imperfections in nanoparticle structure utilized of the purpose of catalysis. On the other hand, seeded mediated growth, thermal decomposition, polyol reduction and biomimetic methods are all bottom top methods [9]. Peptides have been demonstrated to be useful templates to prepare metal catalysts with precise characteristics and high catalytic performance of the NPs [10]-[15]. Key advantages of using peptides include the presentation of a well-defined nucleation site, the prevention of agglomeration during synthesis, room temperature reaction in aqueous solution, and neutral pH [16]. Peptide templated synthesis can control NPs shape, size, and morphology due to the interaction with amino acids contained in the peptide with the metal ion. And the variety of natural and artificial peptide sequences provides numerous opportunities to fabricate the required catalysts [16].

In the past decade, various research articles have been published that have examined the relationship between the specific peptide sequence Pd4 (TSNAVHPTLRHL) and the size, structure, and function of NPs [11] [12] [14]. To date, however, a single report by Mosleh *et al.* hypothesized that lysate containing three copies Pd4 peptide fused to carrier protein Green Fluorescent Protein (GFP) can be used for Pd nanoparticle synthesis in place of purified version and demonstrate that the crude lysate could indeed be used to synthesize NPs with catalytic activity [17]. Continuing the study of purity vs. efficacy, it would be a natural extension of this prior work to compare the properties of enriched $(Pd4)_3$-GFP to these early efforts. Results were obtained in this study from *E. coli* derived proteins enriched by Immobilized Metal Affinity Chromatography (IMAC) and compared to that of Mosleh *et al.* 2019.

2. Experimental Methods

2.1. Plasmid Construction and Protein Expression

SnapGene software was utilized to design a pET-based vector to express a fusion protein between Pd4 and GFP extended by 6 histidine residues. The plasmid also contained DNA elements to permit isopropyl-β-D-1-thiogalactopyranoside (IPTG) (Bio Basic) induction and ampicillin resistance. The DNA of the fused protein was purchased from Integrated DNA Technologies IDT and cloned into pET-22-b (+) (Invitrogen). BL21 *E. coli* strain and restriction enzymes EcoRI and NcoI were purchased from New England Biolabs inc. Expression in *E. coli* BL21 was performed in Lysogeny broth (LB) media. A mixture of autoclaved 500 ml LB media was inoculated with 3 ml of the incubated overnight growth. At 0.8 optical density (OD), growth culture was induced with IPTG. After induction, the growth mixture was incubated for 4 hours at 37˚C and 200 rpm. The antibiotic of 0.1 mg/ml concentration was utilized [18].

2.2. Cell Lysate Preparation

A Beckman Coulter Allegra X-15R centrifuge was employed for 45 minutes at 4˚C and 4500 (×g) rcf to separate cells from spent broth. After cell recovery by

centrifugation, the cells were resuspended in 10 mM phosphate buffer and the ratio of cell pellet to phosphate buffer ratio was 10 ml of buffer to 1 L of obtained cell. Resuspended cells were lysed with Qsonica sonicator at 40% amplitude, 5 seconds run, and pulse for 15 minutes in an ice bath. After sonication, the liquid supernatant was first centrifuged for 45 minutes at 4˚C and 4500 (×g) rcf and further separation with minispin plus centrifuge at 14.1 rcf for 5 minutes [18].

2.3. Protein Purification

The prepared lysate was filtered through a 0.20 um filter. A 5 ml HiTrap IMAC FF column from GE Healthcare-Bio-Sciences (Uppsala, Sweden) was charged with nickel sulfate and washed with water to remove unbound metal ions. For efficient loading and binding, the column was equilibrated with 10 mM of buffer A (sodium phosphate buffer), pH 7.2 - 7.4. After equilibration with buffer A, the prepared lysate was loaded at a flow rate of 0.5 ml/min. An IMAC step gradient was performed for the elution of target protein using buffer B (250 mM imidazole in 10 mM of sodium phosphate buffer) with a pH between 7.2 - 7.4.

2.4. SDS-PAGE Analysis

Proteins were mixed with 2× loading dye, which contains 5% of 2-mercaptoethanol. The samples were denatured by heating for 5 minutes at 95˚C. The electrophoresis chamber (Bio-Rad) was filled with SDS-PAGE running buffer and ran at 180 volts for 50 minutes. After which, the gel was rinsed gently with deionized water, placed in a Comassie blue staining buffer for 30 minutes, and placed in a destaining buffer (75 ml acetic acid, 75 ml methanol, and 850 ml deionized water) overnight.

2.5. Western Blotting

Transfer buffer (1× Towbin with 20% methanol) is used in which the stacking unit is placed. Western blotting was performed for 2 hours at 150 V and 74 mA. After blotting, the nitrocellulose membrane was immersed in 5% skim tris-buffer saline (TBS) (20 ml of 0.5% TBS-Tween and 1 g of skim milk) for 30 minutes to block the non-specific site [19]. The membrane was washed overnight in TBS-T buffer (2 uL of His-tag protein (abcam) and 6 ml of 0.2% bovine serum albumin (BSA) solution). The next day, the nitrocellulose membrane was washed three times for 3 minutes, with TBS-T Tween to remove excess antibodies [19]. After washing, 2 ml of One-step NBT/BCIP (Thermo Fischer Scientific) was added to the membrane and frequently pipetted all over the membrane until the band was detected. After detection was observed, deionized water was used to quench reaction to prevent further darkening of the nitrocellulose membrane [19].

2.6. Palladium Nanoparticle Synthesis

At room temperature, the synthesis of nanoparticles was performed using the

concentrated pure fraction derived from IMAC and the clarified lysate. To fabricate nanoparticles from the concentrated fractions, 750 µL of deionized water, 10 µL of the chromatography fraction, 0.16 mg of potassium tetrachloropalladate (II) (MilliporeSigma) were combined and mixed for 30 min in a 1.5 mL microcentrifuge tube. After the 30 min had elapsed, 1.5 mg of sodium borohydride ($NaBH_4$) (MilliporeSigma) was added as a reduction agent. The synthesized nanoparticles were analyzed using FEI Titan 80 - 300 transmission electron microscopy (TEM) and ImageJ software.

2.7. Catalytic Analysis

A Suzuki-Miyaura reaction was employed to test the catalytic activity of the Pd nanoparticles fabricated from pure $(Pd4)_3$-GFPuv. Into a stirred solution of phenyl benzoic acid and iodobenzoic acids (0.1 mmol, 1.0 equiv), boronic acid (0.12 mmol, 1.2 equiv.) and catalyst (0.25 umol %) in 1ml of EtOH and deionized H_2O (1:1 ratio), and potassium carbonate (K_2CO_3) (0.3 mmol, 3 equiv.) were added at 80˚C for 100 minutes [8]. High pressure liquid chromatography was utilized to quantify the catalytic reaction in increments of 10 minutes. The standards used for the HPLC analysis were the reactants (iodobenze and phenylboronic acid) and the product (biphenyl).

3. Results

3.1. Cloning

Figure 1 presents the plasmid map and translated amino acid sequence of the fusion protein. Plasmid pSAH is comprised of 6341 nucleotides containing the gene for ampicillin resistance and IPTG-inducible cassette. When correctly translated, the immature target protein contains a pelB leader sequence for periplasmic localization and once cleaved begins with an N-terminal methionine. Three copies of Pd4 are separated by the sequence Gly-Gly-Gly-Gly and are fused to the 244 amino acids of GFPuv (Clontech). *E. coli* harboring the plasmid and expressing the fusion protein were green under UV light.

3.2. Chromatography and Protein Identification

IMAC was used to fractionate *E. coli* lysate containing the fusion protein. Figure 2(a) is a representative chromatogram from one chromatography run. Three major peaks are observed, two of which during the imidazole gradient, with the final peak fluorescent green under UV light (Figure 2(b)). To detect the presence of the target protein SDS-PAGE and Western Blotting were employed. Both indicated the expected molecular weight of 32 kDa which represents the total weight of the fusion protein as shown in Figure 3(a) and Figure 3(b). Relative fluorescence intensity (RFI) of pooled concentrated target protein and lysate was determined to be 9500 and 2287, respectively. The obtained RFI showed that the purified pooled fraction is four times more enriched than the lysate.

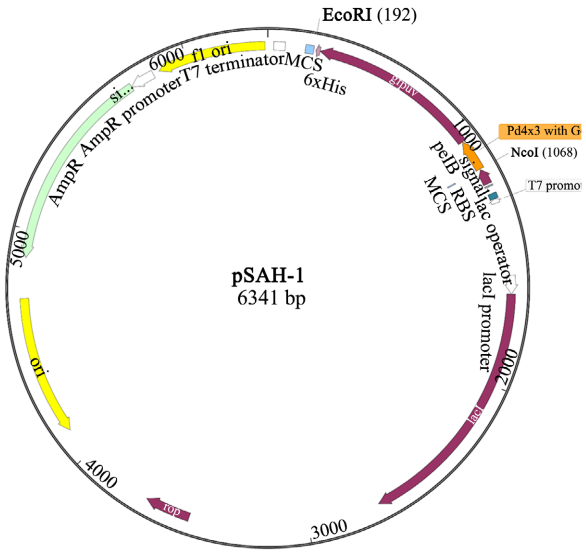

MGTSNAVHPTLRHLGGGGTSNAVHPTLRHLGGGGTSNAVHPTLRHLMSKGEELFTGVVPIL

VELDGDVNGHKFSVSGEGEGDATYGKLTLKFICTTGKLPVPWPTLVTTFSYGVQCFSRYPDHMKRHDFFKSAMPEGYV

QERTISFKDDGNYKTRAEVKFEGDTLVNRIELKGIDFKEDGNILGHKLEYNYNSHNVYITADKQKNGIKANFKIRHNIEDG

SVQLADHYQQNTPIGDGPVLLPDNHYLSTQSALSKDPNEKRDHMVLLEFVTAAGITHGMDELYKHHHHHH

Figure 1. Plasmid map and amino acid sequence of fusion product. Pd4 is indicated by larger font, and GFPuv is underlined.

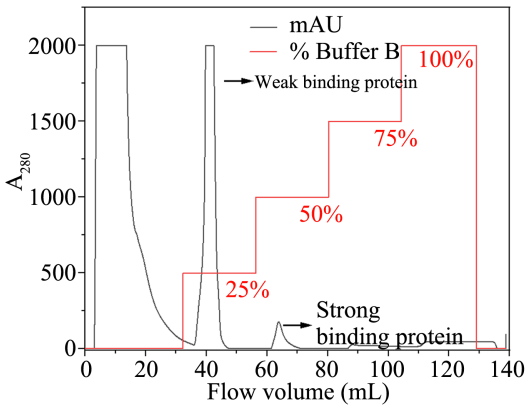

(a)

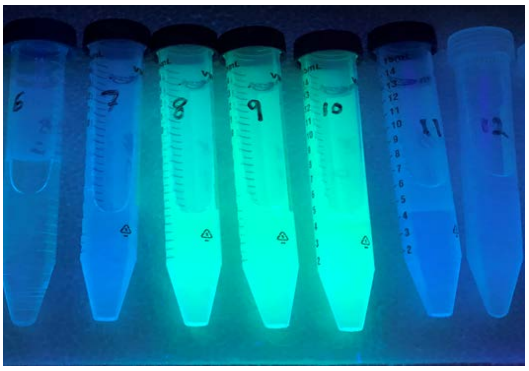

(b)

Figure 2. (a): FPLC Chromatogram showing the elution of weak and strong binding proteins. The chromatogram showed peaks at 62.5 mM and 125 mM concentration of imidazole. The former peak and latter peaks signify the binding of weak and strong binding proteins respectively on the ligand of the column; (b): fluorescence showing eluted fractions of target protein. The elution of the purified fraction at 125 mM (50%) of imidazole with the confirmation of excitation with blue light showed the presence of $(Pd4)_3$ tagged with GFP.

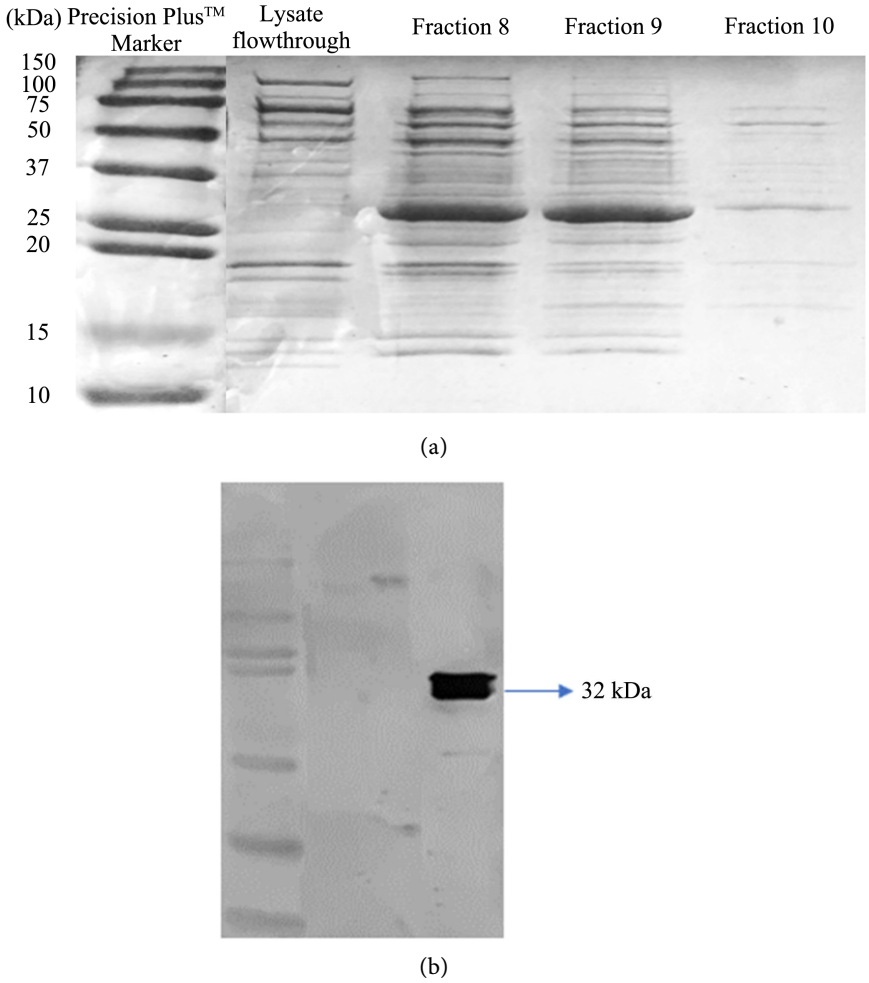

Figure 3. (a): SDS Page Gel and Nitrocellulose membrane of western blotting. Precision Plus ™ marker; lysate flowthrough; 8, 9, and 10-fraction containing GFP tagged Pd4 protein; (b): to detect the presence of protein SDS-PAGE and Western Blotting were employed. Both indicated the expected molecular weight of 32 kDa which represents the total weight of fused protein.

3.3. Nanoparticle Synthesis and Suzuki-Miyaura, Nanoparticle Catalyzed Reaction

The TEM image in **Figure 4** shows the fabricated palladium nanoparticles with an average diameter of 2.44 nm. This image shows the absence of nanoparticle agglomeration which would occur if the NPs were synthesized with *E. coli* lysate or *E. coli* lysate containing GFP-His6. The area of the particles was obtained with ImageJ software from the TEM images and the formula of

$$d = 2X\sqrt{A/\pi}$$

was used to calculate the diameter. The catalytic activity of the synthesized nanoparticles was examined using the optimized model reaction for Suzuki-Miyaura C-C coupling reaction. This yielded a turnover frequency (TOF) of 33,000 hr^{-1} which, when factoring in the amount of protein added to the reaction, gave a value of 65,000 hr^{-1}·$umol^{-1}$ protein.

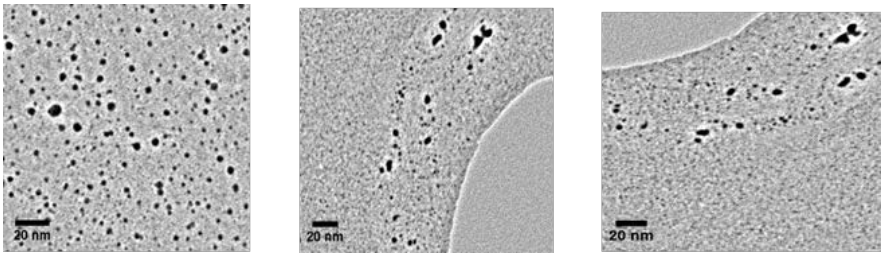

(a)

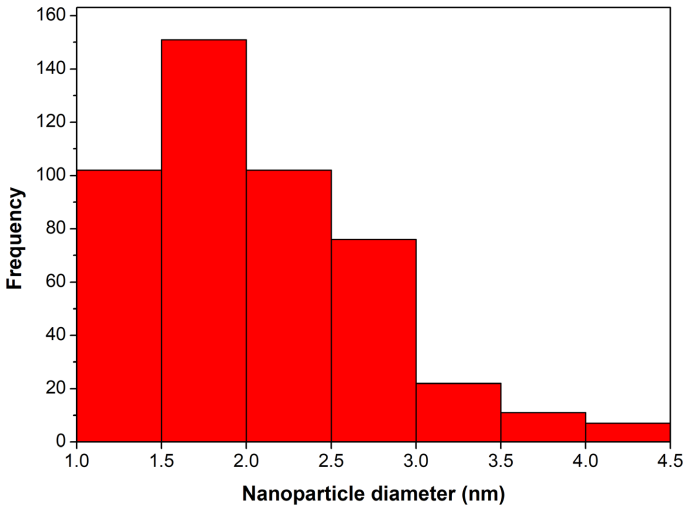

(b)

Figure 4. (a): TEM images of NP fabricated with purified protein; (b): histogram of Size distribution of NP synthesized from IMAC purified protein.

4. Discussion

Providing the Pd4 sequence for nanoparticle synthesis by fusing it to the N-terminus of GFP was first postulated by Tejada *et al.* where it was shown that a crude lysate from *E. coli* could successfully be used to create nanoparticles of palladium [20]. The work was later continued by Mosleh *et al.* who quantified the catalytic activity of palladium nanoparticles on 12 model Suzuki-Miyaura reactions, including the one used to characterize IMAC-enriched materials of this study. Similar to the other reports, microbially-derived Pd4 is easily obtained via fermentation and is favorably competitive when compared to the cost and complexity of the use of chemical synthesis for peptide manufacture. In this study, IMAC was used to provide an enriched sample of three copies of Pd4 fused to the N-terminus of GFPuv. Short stretches of glycine were used to space the three copies apart, motivated by prior examples of fusion protein construction [21] [22] [23]. Compared to other means of luminescent detection involving the addition of an exogenous substrate, GFP requires irradiation by UV or blue light, which provides excellent means of monitoring gene expression and protein localization in cells [24]. Similarly, GFP is used as a fusion tag to either the amino or carboxyl end [25] [26].

IMAC enrichment in a single step provided a sample four times enriched when

compared to the crude lysate. Tejada *et al.* prepared a similar fusion via ion exchange chromatography with a fusion protein content of about 30%; a similar value was obtained here (28%). All preparations of nanoparticle regardless of crude, enriched by ion exchange chromatography, or in the case of this report enriched by IMAC produce palladium nanoparticles on the order of 2.4 nm, indicating a high degree of fidelity by Pd4 as a biotemplate.

Although the NPs are on the same order of size, when one compares the catalytic activity of nanoparticles formed with crude versus IMAC enriched biotemplate an interesting story emerges. This study employed half of the loading of palladium catalyst employed by Imann *et al.*, which was 0.25 μmol% instead of 0.50 μmol%. This yielded a turnover frequency (TOF) of 33,000 hr^{-1} which is 3× more than that obtained by Imann *et al.* Specific TOF of Pd NP fabricated from IMAC purification is 65,000 hr^{-1}·μmol^{-1}, while that from crude lysate is 13,000 hr^{-1}·μmol^{-1}. This increase in specific TOF indicates other proteins present in the mixture can affect the C-C coupling reaction.

5. Conclusions

This paper illustrates the fabrication of palladium nanoparticles with purified peptide templates. It also shows that the purification of protein is advantageous because of the significant increase in palladium nanoparticle Suzuki-Miyaura catalytic activity. This work poses that to obtain an increased catalytic activity for palladium nanoparticles synthesized by palladium metal binding metal peptide, protein purification step is necessary. The proposed explanation to the higher turnover frequency is that the purified metal-binding protein is unencumbered by other metalloproteins or those that simply bind metal ions, which provides significantly more selective surface area for catalytic activities.

The apparent limitation of achieving an enriched metal binding protein for NP synthesis is the cost and time intensive nature of the IMAC purification process. A cost benefit analysis is necessary to examine the short- or long-term benefits of NP. The future prospect of this contribution will involve the extensive analysis of Pd NP derived from enriched metal binding protein in comparison to NP fabricated from lysate to examine the comparative morphology of both NPs. Also, the performance of NP in catalysis of C-C reaction to produce anticancer precursor of Tykerb and water treatment will be examined.

Acknowledgements

The authors wish to thank Dearl Peache and Tammy Lutz-Rechtin for their help. Microscopy assistance by Dr. Mourad Benamara was greatly appreciated. Funding was provided by the University of Arkansas.

Conflicts of Interest

The authors declare no conflicts of interest regarding the publication of this paper.

References

[1] Odularu, A.T. (2018) Metal Nanoparticles: Thermal Decomposition, Biomedicinal Applications to Cancer Treatment, and Future Perspectives. *Bioinorganic Chemistry and Applications*, **2018**, Article ID: 9354708. https://doi.org/10.1155/2018/9354708

[2] Memon, H., Yasin, S., Khoso, N.A. and Memon, S. (2016) Study of Wrinkle Resistant, Breathable, Anti-UV Nanocoated Woven Polyester Fabric. *Surface Review and Letters*, **23**, Article ID: 1650003. https://doi.org/10.1142/S0218625X16500037

[3] Memon, H. and Kumari, N. (2016) Study of Multifunctional Nanocoated Cold Plasma Treated Polyester Cotton Blended Curtains. *Surface Review and Letters*, **23**, Article ID: 1650036. https://doi.org/10.1142/S0218625X16500360

[4] Memon, H., Yasin, S., Ali Khoso, N. and Hussain, M. (2015) Indoor Decontamination Textiles by Photocatalytic Oxidation: A Review. *Journal of Nanotechnology*, **2015**, Article ID 104142. https://doi.org/10.1155/2015/104142

[5] Memon, H., Kumari, N., Jatoi, A.W. and Khoso, N.A. (2017) Study of the Indoor Decontamination Using Nanocoated Woven Polyester Fabric. *International Nano Letters*, **7**, 1-7. https://doi.org/10.1007/s40089-016-0194-7

[6] Memon, H., Wang, H., Yasin, S. and Halepoto, A. (2018) Influence of Incorporating Silver Nanoparticles in Protease Treatment on Fiber Friction, Antistatic, and Antibacterial Properties of Wool Fibers. *Journal of Chemistry*, **2018**, Article ID: 4845687. https://doi.org/10.1155/2018/4845687

[7] Chen, W.X., Yu, J.S., Hu, W., *et al.* (2016) Titanate Nanowire/NiO Nanoflake Core/Shell Heterostructured Nanonanocomposite Catalyst for Methylene Blue Photodegradation. *RSC Advances*, **6**, 67827-67832. https://doi.org/10.1039/C6RA13744J

[8] Mosleh, I., Shahsavari, H.R., Beitle, R. and Beyzavi, M.H. (2020) Recombinant Peptide Fusion Protein-Templated Palladium Nanoparticles for Suzuki-Miyaura and Stille Coupling Reactions. *ChemCatChem*, **12**, 2942-2946. https://doi.org/10.1002/cctc.201902099

[9] Xiong, Y. and Lu, X. (2015) Metallic Nanostructures: From Controlled Synthesis to Applications. Springer International Publishing, Berlin. https://doi.org/10.1007/978-3-319-11304-3

[10] Pacardo, D.B., Sethi, M., Jones, S.E., *et al.* (2009) Biomimetic Synthesis of pd Nanocatalysts for the Stille Coupling Reaction. *ACS Nano*, **3**, 1288-1296. https://doi.org/10.1021/nn9002709

[11] Coppage, R., Slocik, J.M., Sethi, M., *et al.* (2010) Elucidation of Peptide Effects That Control the Activity of Nanoparticles. *Angewandte Chemie—International Edition*, **49**, 3767-3770. https://doi.org/10.1002/anie.200906949

[12] Coppage, R., Slocik, J.M., Briggs, B.D., *et al.* (2012) Determining Peptide Sequence Effects That Control the Size, Structure, and Function of Nanoparticles. *ACS Nano*, **6**, 1625-1636. https://doi.org/10.1021/nn204600d

[13] Bhandari, R., Coppage, R. and Knecht, M.R. (2012) Mimicking Nature's Strategies for the Design of Nanocatalysts. *Catalysis Science & Technology*, **2**, 256-266. https://doi.org/10.1039/C1CY00350J

[14] Coppage, R., *et al.* (2013) Exploiting Localized Surface Binding Effects to Enhance the Catalytic Reactivity of Peptide-Capped Nanoparticles. *Journal of the American Chemical Society*, **135**, 11048-11054. https://doi.org/10.1021/ja402215t

[15] Yu, L., ur Rahman Memon, H., Bhavsar, P.S. and Yasin, S. (2016) Fabrication of Alginate Fibers Loaded with Silver Nanoparticles Biosynthesized via Dolcetto Grape

Leaves (*Vitis vinifera* cv.): Morphological, Antimicrobial Characterization and In Vitro Release Studies. *Materials Focus*, **5**, 216-221. https://doi.org/10.1166/mat.2016.1317

[16] Wang, W., Anderson, C.F., Wang, Z., *et al.* (2017) Peptide-Templated Noble Metal Catalysts: Syntheses and Applications. *Chemical Science*, **8**, 3310-3324. https://doi.org/10.1039/C7SC00069C

[17] Mosleh, I., Benamara, M., Greenlee, L., Beyzavi, M.H. and Beitle, R. (2019) Recombinant Peptide Fusion Proteins Enable Palladium Nanoparticle Growth. *Materials Letters*, **252**, 68-71. https://doi.org/10.1016/j.matlet.2019.05.080

[18] Ibinola, S. and Beitle, B. (2021) Recombinant Production and Purification of Green Fluorescent Protein (GFP)-Fused Metal Binding Protein for Palladium Nanoparticle Synthesis. Ann Arbor. https://www.proquest.com/dissertations-theses/recombinant-production-purification-green/docview/2634873355/se-2?accountid=8361

[19] Scholarworks@uark, S. and Aljewari, H. (2019) Production and Purification of Basic Fibroblast Growth Factor Production and Purification of Basic Fibroblast Growth Factor Fused to two Collagen Binding Domains Expressed in *E. coli* BL21 Fused to Two Collagen Binding Domains expressed in *E. coli* BL21 Using Flask and Fed-Batch Using Flask and Fed-Batch. https://scholarworks.uark.edu/etd/3521

[20] Tejada-Vaprio, R., *et al.* (2020) Recombinant Peptide Fusion Construction for Protein-Templated Catalytic Palladium Nanoparticles. *Biotechnology Progress*, **36**, e2956. https://doi.org/10.1002/btpr.2956

[21] Riggs, P. (2013) Fusion Protein. In: *Brenner's Encyclopedia of Genetics*, 2nd Edition, Elsevier Inc., Amsterdam, 134-135. https://doi.org/10.1016/B978-0-12-374984-0.00565-9

[22] Falke, J.J. and Corbin, J.A. (2004) Affinity Tags for Protein Purification.

[23] Rizk, M., Antranikian, G. and Elleuche, S. (2012) End-to-End Gene Fusions and Their Impact on the Production of Multifunctional Biomass Degrading Enzymes. *Biochemical and Biophysical Research Communications*, **428**, 1-5. https://doi.org/10.1016/j.bbrc.2012.09.142

[24] Chalfie, M., Tu, Y., Euskirchen, G., Ward, W.W. and Prashert, D.C. (1994) Green Fluorescent Protein as a Marker for Gene Expression. *Science* (1979), **263**, 802-805. https://doi.org/10.1126/science.8303295

[25] Tsien, R.Y. (1998) The Green Fluorescent Protein. *Annual Review of Biochemistry*, **67**, 509-544. https://doi.org/10.1146/annurev.biochem.67.1.509

[26] Shimomura, O. (1979) Structure of the Chromophore of Aequorea Green Fluorescent Protein. *FEBS Letters*, **104**, 220-222. https://doi.org/10.1016/0014-5793(79)80818-2